# Generation of downshifted oscillations in the electron foreshock: A loss-cone instability

V. V. Lobzin,[1] V. V. Krasnoselskikh,[1] S. J. Schwartz,[2] Iver Cairns,[3] B. Lefebvre,[2] P. Décréau,[1] and A. Fazakerley[4]

Received 19 May 2005; revised 26 July 2005; accepted 3 August 2005; published 16 September 2005.

[1] Measurements performed aboard Cluster spacecraft near Earth's bow shock on 24 January 2001 provide convincing evidence of a loss-cone feature within the electron foreshock region. This feature is formed by suprathermal electrons with energies 15–45 eV and pitch angles 130°–150° and is always accompanied by electrostatic waves with frequencies well below the local plasma frequency. An instability analysis shows that these downshifted oscillations can result from a loss-cone instability of electron cyclotron modes rather than from the beam instability as previously suggested.
**Citation:** Lobzin, V. V., V. V. Krasnoselskikh, S. J. Schwartz, I. Cairns, B. Lefebvre, P. Decreau, and A. Fazakerley (2005), Generation of downshifted oscillations in the electron foreshock: A loss-cone instability, *Geophys. Res. Lett.*, *32*, L18101, doi:10.1029/2005GL023563.

## 1. Introduction

[2] High frequency fluctuating electric fields near the Earth's bow shock were reported first time by *Fredricks et al.* [1968]; using the plasma wave experiment aboard OGO 5, they found that upstream of the shock wave the electric field spectra contained a significant peak near the local plasma frequency, $f_{pe}$, while the magnetic field was quiet. Later on, *Scarf et al.* [1971] associated these wave bursts with the fluxes of electrons which move upstream from the bow shock and have energies of 700–800 eV. *Filbert and Kellogg* [1979] hypothesized that these waves are generated by a beam-like instability and suggested a time-of-flight mechanism to a bump-on-tail in the electron reduced distribution function, later refined by *Cairns* [1987]. *Feldman et al.* [1983] observed field-aligned beams in two-dimensional distributions measured at the foreshock boundary. From three-dimensional measurements of electron distributions, *Fitzenreiter et al.* [1984] found that near the foreshock boundary the reduced distribution functions can have a bump-on-tail which is necessary for instability to occur.

[3] *Etcheto and Faucheux* [1984] and *Lacombe et al.* [1985] performed detailed statistical studies of electrostatic waves that were observed upstream of the Earth's bow shock by ISEE 1 and had frequencies near $f_{pe}$. Using the relaxation sounder data, they found intense narrow-band noise at $f_{pe}$ near the leading edge of the foreshock, the bandwidth being a few percent of $f_{pe}$; deep within the foreshock the wave intensity is smaller and the spectra have larger width, up to 0.3 $f_{pe}$. *Etcheto and Faucheux* [1984] argued that there are two kinds of wide-band spectra, one with a low frequency cut-off at $f_{pe}$ and another one with symmetrically distributed intensity above and below $f_{pe}$. *Lacombe et al.* [1985] wrote that on average the peak frequency of the broad band noise is higher than $f_{pe}$, the difference between these two frequencies being as large as 5 kHz. Using data from plasma wave instruments on ISEE 1 and ISEE 2, *Fuselier et al.* [1985] found that the wave frequency varies within a considerably larger range, from 0.1 $f_{pe}$ to 1.1 $f_{pe}$. For one bow shock crossing the electron reduced distribution function measured close to the foreshock edge was shown to have a bump-on-tail feature; as the spacecraft moved deeper into foreshock, the peak corresponding to energetic electrons transformed into a plateau and finally disappeared [*Fuselier et al.*, 1985].

[4] To explain the observations, *Lacombe et al.* [1985], *Fuselier et al.* [1985], *Cairns and Fung* [1988], and *Dum* [1990] assume that both narrow-band and wide-band waves are generated due to a combination of the plasma-beam interaction with the time-of-flight mechanism of the beam formation, and that wide-band waves can be considered as beam modes. However, for the instability of downshifted waves to occur, the beam velocity must fall into the range of bulk thermal velocities for which a Landau damping by thermal electrons is significant; hence, the spread of the beam must be very small [*Cairns and Fung*, 1988; *Dum*, 1990]. Such low-energy, weak, and narrow beams are extremely difficult to observe on the background of the bulk and up to now there is no convincing experimental evidence that such beams exist. On the other hand, both from the theory [*Leroy and Mangeney*, 1984; *Wu*, 1984] and numerical simulations [*Fitzenreiter et al.*, 1990] of energization of electrons by the quasiperpendicular shock it follows that the reflected electrons should form a loss-cone-like feature which was also observed experimentally in several snapshots of electron distribution measured upstream of the high-$\beta$ supercritical quasiperpendicular Earth's bow shock [*Scudder et al.*, 1986]. Similar feature was also observed upstream of the comet Halley bow shock as enhanced low energy electron fluxes which peak at 90° pitch angles and were interpreted as a consequence of adiabatic heating by the magnetic field increase resulting from the cometary mass loading [*Larson et al.*, 1992].

[5] In this paper we present convincing experimental evidence that the loss-cone formed by suprathermal elec-

[1]LPCE/CNRS-Université d'Orléans, Orléans, France.
[2]Imperial College London, London, UK.
[3]University of Sydney, Sydney, New South Wales, Australia.
[4]Mullard SSL, University College London, Surrey, UK.


0094-8276/05/2005GL023563

trons exists in the electron foreshock and suggest a new mechanism of generation of downshifted oscillations due to loss-cone instability.

## 2. Observations of Electrostatic Waves and Electron Distributions in the Foreshock

[6] Here we study electron distributions and downshifted waves observed upstream of the Earth's bow shock by Cluster spacecraft on 24 January 2001 at 07:05:00–07:09:00 UT. The data used were obtained from two experiments, namely the Plasma electron and current analyser (PEACE) and Waves of high frequency and sounder for probing of density by relaxation (WHISPER) [*Johnstone et al.*, 1997; *Décréau et al.*, 1997].

[7] The bow shock under study can be considered as a typical quasiperpendicular, supercritical, high-$\beta$, and high-Mach-number shock. Indeed, from the available experimental data the following estimates were obtained: upstream $\beta_e = 1.7$, the angle between the shock normal and the upstream magnetic field is $\theta_{Bn} = 81°$, and the Alfvén and fast mode Mach numbers are $M_A = 10$ and $M_f = 5$.

[8] Since the frequencies of the waves studied are much larger than the ion plasma frequency, their properties are related mainly to the electron distributions. The key question is: what are the typical features of electron particle distributions associated with the downshifted waves? To answer this question, we analyzed a series of electron distributions and the corresponding wave spectra. Since the time resolution of WHISPER is much higher than that of PEACE, the electric field spectra were averaged over the corresponding 4 s time intervals required to obtain each electron distribution.

[9] Figure 1 shows two spectra of the electric field fluctuations (bottom panel) and the corresponding electron energy distributions (top panel) measured aboard Cluster-3. The chosen representation of the electron distributions combines the dependencies of the differential electron fluxes upon the energy and the pitch angle. Since the spacecraft potential is non-vanishing, the electron energies should be decreased by approximately 6–7 eV. In the wave spectrum obtained near the foreshock boundary during 07:04:29–07:04:33 UT (Figure 1a) there is a well-pronounced peak near $f_{pe} \approx 26$ kHz. The corresponding electron distribution has a characteristic bump-on-tail feature at energies ~100–300 eV and pitch angles near 180°. Figure 1b shows the wave spectrum and electron distribution obtained deep in the foreshock during 07:05:13–07:05:17 UT. The spectrum contains two peaks, one narrow and one broad. The narrow peak is located near $f_{pe}$, while the wider one corresponds to the downshifted waves and is maximum at 15 kHz. The power density of downshifted oscillations is smaller than that of Langmuir waves, while the frequency band they occupy is considerably wider. The corresponding electron distribution function has no bump-on-tail. Instead, the yellow-orange colored cones resembling "rabbit ears" are observed in the energy range 10–45 eV in the lower part, corresponding to electrons moving upstream away from the shock. These electron fluxes are not aligned with the magnetic field; the angle between their direction and magnetic field is about 150°, the maximum fluxes being detected in the energy range 15–27 eV.

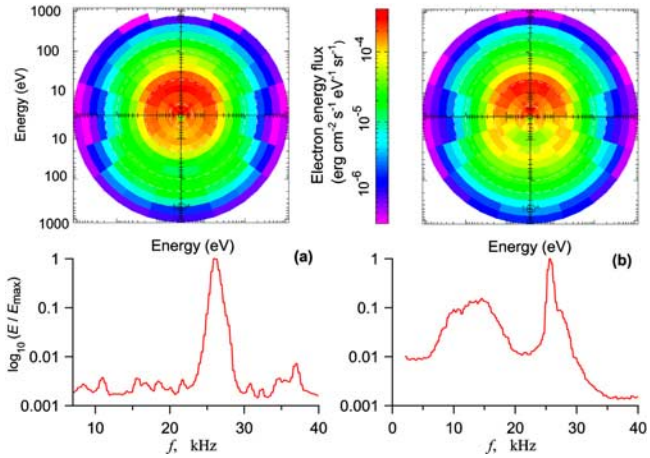


**Figure 1.** Electron differential energy flux versus energy and pitch angle (top panel) and the corresponding electric field spectra (bottom panel) measured (a) near the forward edge of the electron foreshock and (b) deeper. The differential electron energy fluxes are color coded. The pitch angles are measured from the upward direction of the vertical axis, while the logarithm of energy is proportional to the distance from the coordinate origin.

[10] The spectra and electron distributions shown in Figure 1 are typical for the studied crossing of the electron foreshock. We summarize the experimental findings as follows. Downshifted oscillations with considerable frequency shifts with respect to the $f_{pe}$ are observed within the foreshock, far enough from its upstream boundary, and are always accompanied by a loss-cone feature, while there is no observable bump-on-tail in this region. On the other hand, not far from the forward edge of the electron foreshock, both loss-cone and downshifted oscillations vanish and only field-aligned beams and oscillations near $f_{pe}$ are observed.

[11] These facts can be considered as a strong argument in favor of a loss-cone instability for downshifted oscillations rather than a beam instability. If a plasma does not contain any electron beam, in the range between electron and ion plasma frequencies there exist only electron cyclotron modes, which propagate almost across the magnetic field.

## 3. Loss-Cone Instability of Electrostatic Electron Cyclotron Waves

[12] To provide a theoretical explanation for the generation of downshifted oscillations within the electron foreshock, we assume that these oscillations correspond to electrostatic electron cyclotron waves. Let the plasma contain three electron components, i.e., cold core, hot halo, and solar wind electrons reflected from/accelerated by the shock front and responsible for "rabbit ears" loss-cone feature shown in Figure 1b. We assume further that the plasma is homogeneous and the fluid velocities of ions, cold and hot electrons are zero in the reference frame chosen.

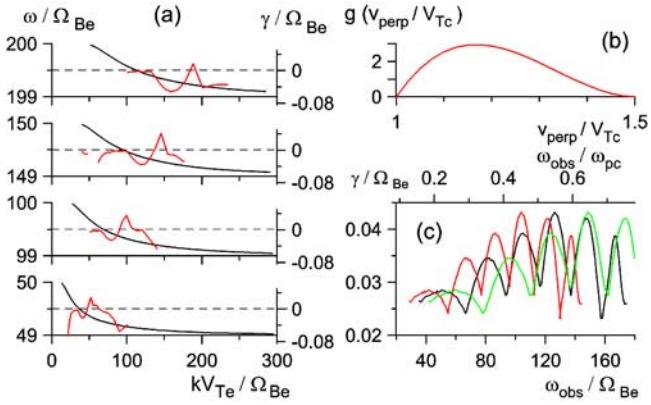


**Figure 2.** Instability of electron cyclotron waves due to loss-cone distribution of reflected/accelerated electrons. (a) The complex frequency of several electron cyclotron modes as a function of wave number. The black curves represent $\omega/\Omega_{Be}$ (left axis), while the normalized growth rates $\gamma/\Omega_{Be}$ are shown by red lines (right axis). The wavenumber is multiplied by the thermal electron gyroradius for cold electrons. (b) The shape of the distribution of accelerated electrons versus perpendicular velocity. (c) The dependence of the maximum growth rates as a function of the observed frequency, where $\omega_{obs} = \omega$ (black line) and $\omega_{obs} = \omega \mp k_\perp V_{sw\perp}$ (red and green lines, respectively).

[13] From the PEACE measurements it follows that both hot and cold electrons can be considered as Maxwellian,

$$f_{c,h}(\mathbf{v}) = \frac{n_{c,h}}{(2\pi)^{3/2} V_{Tc,h}^3} \exp\left(-\frac{\mathbf{v}^2}{2V_{Tc,h}^2}\right),$$

and the ratios of number densities and temperatures of the core and halo electrons don't vary appreciably within the foreshock, typical values being $n_h/n_c = 0.1$ and $T_h/T_c = 8$. In these formulas and in the following, unless otherwise stated, we use a standard notation. Subscripts $c$ and $h$ denote the cold and hot electrons, respectively; the subscript $r$ is used for the reflected electrons; thermal velocities are given by $V_{T\alpha} = (T_\alpha/m_e)^{1/2}$, where $\alpha = c$, $h$, or $r$.

[14] The "rabbit ears" exist within bounded ranges of energies and pitch angles. To model this feature, we can use the distribution of reflected electrons in the following form:

$$f_r(\mathbf{v}) = \frac{n_r\, g\,(v_\perp/V_{Tc})}{(2\pi)^{3/2} V_{Tr} V_{Tc}^2} \exp\left[-\frac{(v_\parallel - V_0)^2}{2V_{Tr}^2}\right], \qquad (1)$$

where $\int_0^{+\infty} g(x)x\,dx = 1$, the shape of this function should be estimated experimentally. From PEACE measurements it follows that $n_r/n_c \simeq 0.03$, the maximum of energy flux due to "rabbit ears" is located in the velocity range 1.1–1.3 $V_{Tc}$ for both cartesian velocity components; the parallel temperature of the reflected electrons lies between the temperatures of cold and hot components, $T_r/T_c \simeq 5$.

[15] The dielectric response function of the plasma can be written as follows:

$$\varepsilon = 1 + \delta\varepsilon_c(\omega, \mathbf{k}) + \delta\varepsilon_h(\omega, \mathbf{k}) + \delta\varepsilon_r(\omega, \mathbf{k}),$$

where $\delta\varepsilon_\alpha$ denotes the contribution of each electron component.

[16] To calculate the growth rate $\gamma$, we use a well-known approximate formula [see, e.g., *Ginzburg*, 1970]

$$\gamma = -\Im\varepsilon(\omega, \mathbf{k}) \Big/ \frac{\partial \Re\varepsilon(\omega, \mathbf{k})}{\partial\omega}.$$

[17] Let us consider the electron cyclotron waves that propagate almost across the magnetic field with $|k_\parallel| V_{Tc} \ll \Omega_{Be}$, while $|k_\parallel| V_{Th,r}$ can have the same order of magnitude as $\Omega_{Be}$, where $\Omega_{Be}$ is the electron gyrofrequency. Since $\omega_{pc} \gg \omega_{ph,r}$, where $\omega_{p\alpha}$ denotes the plasma frequency for each electron component, in this case the contribution of hot and reflected electrons into the real part of the dielectric response function can be neglected and the contribution of cold electrons is given by

$$\Re(\delta\varepsilon_c) = -\frac{\omega_{pc}^2 \Omega_{Be}^2}{k_\perp^2 V_{Tc}^2} \sum_{n=-\infty}^{\infty} \frac{n^2 \Lambda_n\left(k_\perp^2 V_{Tc}^2/\Omega_{Be}^2\right)}{\omega(\omega - n\Omega_{Be})},$$

where $\Lambda_n(x) = I_n(x)\exp(-x)$ [*Ichimaru*, 1973].

[18] Since a Maxwellian distribution can be considered as a special case of distribution like (1), the contribution of all electron components into imaginary part of the dielectric response function can be calculated with the use of the same relationship,

$$\Im(\delta\varepsilon_\alpha) = -\sqrt{\frac{\pi}{2}} \frac{\omega_{p\alpha}^2}{k^2 V_{Tc}^2} \frac{1}{\Delta n_\alpha} \sum_{n=-\infty}^{+\infty} \exp\left[-\frac{1}{2}\left(\frac{n - n_{0\alpha}}{\Delta n_\alpha}\right)^2\right] \cdot \left\{\int_0^\infty J_n^2(\kappa x)\left[\frac{(n - n_{0\alpha}) x g_\alpha(x)}{(V_{T\alpha}/V_{Tc})^2} + n g_\alpha'(x)\right] dx\right\},$$

where $n_{0\alpha} = (\omega - k_\parallel V_{0\alpha})/\Omega_{Be}$, $\Delta n_\alpha = |k_\parallel| V_{T\alpha}/\Omega_{Be}$, and $\kappa = k_\perp V_{Tc}/\Omega_{Be}$.

[19] The results of numerical calculations of both the real part of the wave frequency and growth rate are summarized in Figure 2 in the case when $\omega_{pe}/\Omega_{Be} = 230.5$, $N_r/N_c = 0.03$, $N_h/N_c = 0.10$, $T_{\parallel r}/T_c = 5$, $T_h/T_c = 8$, and $V_0/V_{Tc} = 1$. The top part of the right panel shows the electron distribution profile $g = g(v_\perp/V_{Tc})$ used in the calculations; in accordance with the experimental data we suppose that the "rabbit ears" vanish outside the interval $1.0 \le v_\perp/V_{Tc} \le 1.5$. In the left panel shown are the dependencies of the real part of the frequency on wave number for four electron cyclotron modes, together with the corresponding growth rates. The lower plot on the right panel presents the dependence of maximum value of the growth rate versus the frequency. The maximum is calculated with respect to perpendicular wave vector component, while the parallel component is fixed and corresponds to $\Delta n_c = 0.2$.

[20] The results show that the maximum growth rates correspond to the frequency range 0.4–0.7 $\omega_{pe}$, in accordance with observations, and can be as large as 0.04–0.05 $\Omega_{Be}$. The maximum growth rate varies with the frequency, oscillating with a period ~20 $\Omega_{Be}$. However, these oscillations can be smeared out by Doppler shifts. Indeed, assume that there is no preferential value of the azimuth angle of the wave vector. In this case observed frequency for given $k_\perp$ can vary within the range $\omega - k_\perp V_{sw\perp} \le \omega_{obs}$

$\leq \omega + k_\perp V_{sw\perp}$, where $V_{sw} \simeq 0.18\ V_{Tc}$ is the solar wind velocity. The curves corresponding to the ends of this interval are also shown in Figure 2, thereby confirming that the Doppler shift can be large enough to smear out the oscillations of the growth rate and form a smooth wide maximum.

## 4. Discussion and Conclusions

[21] It was commonly believed that narrow-band Langmuir waves at the forward edge of the foreshock, as well as wide-band upshifted and downshifted oscillations deep in the foreshock are generated by a beam-like feature formed by energetic electrons [see, e.g., *Lacombe et al.*, 1985; *Fuselier et al.*, 1985; *Cairns and Fung*, 1988; *Dum*, 1990]. However, in accordance with the theoretical predictions [*Filbert and Kellogg*, 1979; *Leroy and Mangeney*, 1984; *Wu*, 1984], deep within foreshock the energetic electrons have energies comparable with the thermal one of the bulk population. In this case, for a beam instability to exist the beam should have an extremely narrow velocity spread that makes the beam difficult to observe [*Cairns and Fung*, 1988]. The lack of experimental observations of such beams deep within foreshock makes their existence at least questionable. On the other hand, the shock wave can be considered as a magnetic field barrier reflecting solar wind electrons with large pitch angles; hence, the reflected electrons should have a loss-cone distribution shifted due to acceleration [*Leroy and Mangeney*, 1984; *Wu*, 1984]. This feature was also visible in the electron distributions measured upstream of the Earth and comet Halley bow shocks [*Scudder et al.*, 1986; *Larson et al.*, 1992].

[22] The Cluster measurements reported in this paper provide convincing experimental evidence that a loss-cone feature exists within the extensive region of electron foreshock. For the event considered this feature is formed by suprathermal electrons with energies 15–45 eV and pitch angles 130°–150°. The relative velocity of this population with respect to the bulk population is comparable with the thermal velocity of the bulk, while the observed energy spread of the loss-cone electrons is larger than bulk thermal energy and there is no indication that narrow beams exist.

[23] The observed loss-cone feature is always accompanied by electrostatic waves with frequencies well below the local plasma frequency. The instability analysis shows that these downshifted oscillations can result from a loss-cone instability of electron cyclotron modes rather than a beam instability of the Langmuir and/or beam modes.

[24] **Acknowledgments.** V. V. Lobzin is grateful to the administration of the Region Centre of France and to CNRS for financial support during his stay at LPCE. V. V. Krasnoselskikh and S. J. Schwartz are grateful to CNRS and Royal Society for financial support from collaboration project 12019.

## References

Cairns, I. H. (1987), The electron distribution function upstream from the Earth's bow shock, *J. Geophys. Res.*, *92*, 2315.

Cairns, I. H., and S. F. Fung (1988), Growth of electron plasma waves above and below $f_p$ in the electron foreshock, *J. Geophys. Res.*, *93*, 7307.

Décréau, P. M. E., et al. (1997), Whisper, a resonance sounder and wave analyser: Performances and perspectives for the Cluster mission, *Space Sci. Rev.*, *79*, 157.

Dum, C. T. (1990), Simulation studies of plasma waves in the electron foreshock: The generation of downshifted oscillations, *J. Geophys. Res.*, *95*, 8123.

Etcheto, J., and M. Faucheux (1984), Detailed study of electron plasma waves upstream of the Earth's bow shock, *J. Geophys. Res.*, *89*, 6631.

Feldman, W. C., et al. (1983), Electron velocity distributions near the Earth's bow shock, *J. Geophys. Res.*, *88*, 96.

Filbert, P. C., and P. J. Kellogg (1979), Electrostatic noise at the plasma frequency beyond the Earth's bow shock, *J. Geophys. Res.*, *84*, 1369.

Fitzenreiter, R. J., A. J. Klimas, and J. D. Scudder (1984), Detection of bump-on-tail reduced electron velocity distributions at the electron foreshock boundary, *Geophys. Res. Lett.*, *11*, 496.

Fitzenreiter, R. J., J. D. Scudder, and A. J. Klimas (1990), Three-dimensional analytical model for the spatial variation of the foreshock electron distribution function: Systematics and comparisons with ISEE observations, *J. Geophys. Res.*, *95*, 4155.

Fredricks, R. W., C. F. Kennel, F. L. Scarf, G. M. Crook, and I. M. Green (1968), Detection of electric-field turbulence in the Earth's bow shock, *Phys. Rev. Lett.*, *21*, 1761.

Fuselier, S. A., D. A. Gurnett, and R. J. Fitzenreiter (1985), The downshift of electron plasma oscillations in the electron foreshock region, *J. Geophys. Res.*, *90*, 3935.

Ginzburg, V. L. (1970), *The Propagation of Electromagnetic Waves in Plasmas*, 2nd ed., Elsevier, New York.

Ichimaru, S. (1973), *Basic Principles of Plasma Physics*, Benjamin, White Plains, N. Y.

Johnstone, A. D., et al. (1997), Peace: A plasma electron and current experiment, *Space Sci. Rev.*, *79*, 351.

Lacombe, C., A. Mangeney, C. C. Harvey, and J. D. Scudder (1985), Electron plasma waves upstream of the Earth's bow shock, *J. Geophys. Res.*, *90*, 73.

Larson, D. E., et al. (1992), Electron distributions upstream of the comet Halley bow shock: Evidence for adiabatic heating, *J. Geophys. Res.*, *97*, 2907.

Leroy, M. M., and A. Mangeney (1984), A theory of energization of solar wind electrons by the Earth's bow shock, *Ann. Geophys.*, *2*, 449.

Scarf, F. L., R. W. Fredricks, L. A. Frank, and M. Neugebauer (1971), Nonthermal electrons and high-frequency waves in the upstream solar wind: 1. Observations, *J. Geophys. Res.*, *76*, 5162.

Scudder, J. D., et al. (1986), The resolved layer of a collisionless, high β, supercritical, quasi-perpendicular shock wave: 1. Rankine-Hugoniot geometry, currents, and stationarity, *J. Geophys. Res.*, *91*, 11,019.

Wu, C. S. (1984), A fast Fermi process: Energetic electrons accelerated by a nearly perpendicular bow shock, *J. Geophys. Res.*, *89*, 8857.

I. Cairns, School of Physics, University of Sydney, Sydney, NSW 2006, Australia.

P. Décréau, V. V. Krasnoselskikh, and V. V. Lobzin, LPCE/CNRS-Université d'Orléans, 3A Avenue de la Recherche Scientifique, 45071, Orléans, CEDEX 2, France. (vlobzine@cnrs-orleans.fr)

A. Fazakerley, Mullard SSL, University College London, Holmbury St. Mary, Dorking, Surrey, RH5 6NT, UK. (anf@mssl.ucl.ac.uk)

S. J. Schwartz and B. Lefebvre, Space and Atmospheric Physics, The Blackett Laboratory, Imperial College London, London SW7 2AZ, UK.